Analysis and Design of MESFET Gate Mixers

CARLOS CAMACHO-PEÑALOSA, MEMBER, IEEE, AND COLIN S. AITCHISON

Abstract **—A general and efficient nonlinear/linear analysis of MESFET gate mixers is presented. In the nonlinear analysis, the Newton-Raphson algorithm is used in conjunction with a novel approach for computing partial derivatives required by the Jacobian. The study of conversion gain and stability characteristics of the mixer is based on S-parameter matrix theory. As a result of the analysis, the possibility of improving the conversion gain of X-band MESFET gate mixers by an appropriate choice of the RF drain termination has been theoretically and experimentally demonstrated.**

I. Introduction

THEORETICAL ANALYSIS of MESFET mixer performance provides information by which actual design can be performed and improved. Since the early paper by Pucel *et al.* [1], a good deal of work [2]–[7] has been carried out in order to clarify the functioning of different MESFET mixer configurations. As pointed out by Maas [8], the attempts to analyze these circuits have been of limited accuracy or applicability due to simplifying assumptions on the MESFET large-signal model and/or the nonlinear–linear analysis of its performance. Despite these limitations, some of these works raised the very interesting question of the influence of parasitic terminations on the mixer performance. Only recently, more general approaches removing all or part of these limitations have been published [8], [9]. Nevertheless, these have been used to predict the performance of practical mixers, but no attempt to apply such general methods to the study of the functioning and improvement of the circuits has been made.

In this paper, a general and efficient nonlinear–linear analysis technique for the study of MESFET mixers is presented. The local oscillator injection problem is solved by an improved harmonic balance method [10] where the Newton-Raphson algorithm is used to solve the resulting nonlinear equation system. Partial derivatives required by the Jacobian are computed by a novel approach [10] which drastically reduces the computer time. This approach can be considered as a generalization of that used by Egami [11] to solve the local oscillator problem in Schottky diode mixers. In the linear analysis, an S-parameter matrix is employed to characterize the behavior of the mixer. Therefore, the conversion gain and stability characteristics of the mixer can be easily studied by using standard microwave amplifier design methods.

The technique is applied to the analysis and design of MESFET gate mixers. The functioning of these circuits is clarified and an optimum design criterion based on a proper choice of parasitic terminations is proposed. Theoretical results are supported by measurements on a practical X-band MESFET gate mixer with state-of-the-art performance.

II. MESFET Nonlinear Model

The quasi-static nonlinear model used to simulate the behavior of the MESFET (NE71000) under large-signal conditions is shown in Fig. 1. It contains three elements depending on voltages $v_1(t)$ and $v_2(t)$, namely, $i_m(v_1, v_2)$, $C_{gs}(v_1)$, and $R_i(v_1)$. The instantaneous current $i_c(t)$ through the capacitance C_{gs} is given by

$$i_c(t) = C_{gs}[v_1(t)]\frac{dv_1(t)}{dt} \tag{1}$$

with

$$C_{gs}(v_1) = C_{gs0}\Big/\sqrt{1-\frac{v_1}{\phi}} \qquad \text{for } v_1 < \phi. \tag{2}$$

The resistance $R_i(v_1)$ is defined by [12]

$$R_i(v_1)C_{gs}(v_1) = \tau_i. \tag{3}$$

Thus the voltage $v_i(t)$ across this element is given by

$$v_i(t) = R_i[v_1(t)]i_c(t) = R_i[v_1(t)]C_{gs}[v_1(t)]\frac{dv_1(t)}{dt} = \tau_i\frac{dv_1(t)}{dt}. \tag{4}$$

The dependence of i_m upon v_1 and v_2 is described by the expression proposed by Tajima *et al.* [12]. In order to take into account the time delay between drain current and gate voltage, the instantaneous value of $i_m(t)$ is computed

Manuscript received August 4, 1986; revised March 9, 1987. This work was supported by the British Council, by the Spanish Ministerio de Educación y Ciencia (Fleming award), and by the Spain CAICYT under Project 0348/84.

C. Camacho-Peñalosa was with the Department of Electronics, Chelsea College, now called King's College (KQC), University of London, on leave from Grupo de Electromagnetismo Aplicado, ETSI Telecomunicación, Universidad Politécnica de Madrid, 28040 Madrid, Spain.

C. S. Aitchison was with the Department of Electronics, Chelsea College, now called King's College (KQC), University of London. He is now with ERA Technology, Ltd., Leatherhead, Surrey, KT22 75A, England.

IEEE Log Number 8715006.

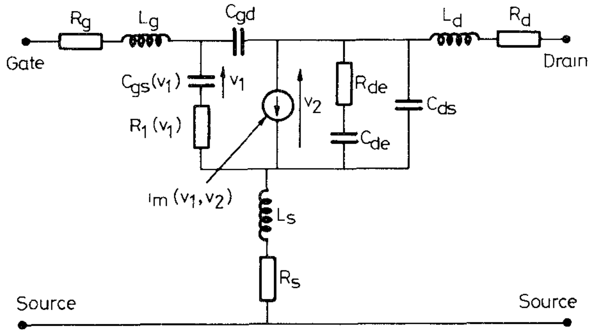

Fig. 1. Large-signal MESFET model. Linear element values are $R_g = R_d = 0$, $R_s = 1.0\ \Omega$, $L_g = L_d = 0.2$ nH, $L_s = 0.06$ nH, $R_{de}^{-1} = 3$ mS, $C_{de} = 0.2\ \mu$F, $C_{ds} = 0.072$ pF, $C_{gd} = 0.035$ pF. Nonlinear element parameter values are $C_{gs0} = 0.37$ pF, $\phi = 0.9$ V, $\tau_i = 2.5$ ps. Parameter values of the nonlinear current generator are given in the caption to Fig. 2.

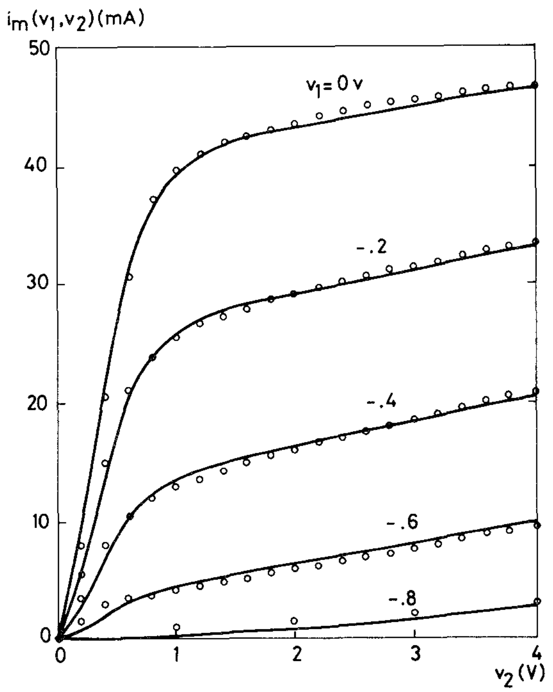

Fig. 2. NE 71000 measured (○) and model-predicted (solid lines) dc characteristics. Parameter values are $a = 6.85$, $b = -2.30$, $m = 4.27$, $p = 0.050$, $V_{p0} = 0.78$ V, $V_{dss} = 1.45$ V, $I_{dsp} = 0.115$ A, $\tau = 2.5$ ps.

using

$$i_m(t) = i_m[v_1(t-\tau), v_2(t)] \tag{5}$$

where τ is a model parameter.

The parameters[1] describing this nonlinear current generator are obtained by fitting the measured dc drain current–voltage characteristics. A comparison of measured and model-predicted dc characteristics is presented in Fig. 2. It should be mentioned that outside the range of v_2 used in the characterization ($v_2 \leqslant 4.0$ V), an extrapolation defined by

$$i_m(v_1, v_2) = i_m(v_1, 4.0) + \left.\frac{\partial i_m}{\partial v_2}\right|_{(v_1, 4.0)} (v_2 - 4.0) \tag{6}$$

was introduced to avoid the incorrect simulation obtained with the expression proposed in [12] and the parameter values given in the caption to Fig. 2.

The remaining elements are considered to be linear. It is assumed that there is no variation of $g_m (= \partial i_m / \partial v_1)$ with frequency, while the frequency sensitivity of $g_d (= \partial i_m / \partial v_2)$ is modeled by the branch $R_{de} - C_{de}$ [13]. The assumption[2] that R_{de} and C_{de} do not depend on v_1 and v_2, as well as the Schottky barrier junction assumption for C_{gs} [8] and the constant-capacitance assumption for C_{gd} [8], is valid as long as the device remains in the saturation region. On the other hand, the validity of the model is also limited to values of $v_1(t)$ lower than +0.5 V (approximately) because the nonlinear conductance of the Schottky barrier (in parallel with C_{gs}) has not been considered.

Because of its high value (0.2 μF typically), C_{de} cannot be determined from microwave S-parameter measurements and therefore low-frequency measurements are required [13]. However, if the model is going to be used only at microwave frequencies, it is not necessary to know its exact value. At these frequencies this capacitance presents a negligible impedance when compared to R_{de}; therefore, it can be considered as a short circuit. The values for the remaining elements have been obtained by computer-fitting the calculated S parameters to the measured data in the 2–18-GHz range.

In spite of all its limitations, the close agreement between experimental and model-predicted results described in Section VI demonstrates that the model can be considered to be accurate enough to simulate the performance of MESFET gate mixers.

III. Nonlinear Analysis

If the nonlinear model described in Section II is used to simulate the large-signal behavior of the MESFET, the problem of computing the local oscillator waveforms in the mixer is reduced to the calculation of the steady-state response of the circuit represented in Fig. 3. It is considered that the LO signal is fed into the device through the gate port.

A. Nonlinear Equation System and Its Solution

Following [10], voltages $v_1(t)$ and $v_2(t)$, which control the nonlinear elements and are not linearly related, are chosen to be unknowns in order to take full advantage of the linear elements in the circuit.

Under large-signal LO excitation, all currents and voltages in the circuit become, in general, periodic functions of time and can consequently be represented by their Fourier series

$$x(t) = \sum_{k=-\infty}^{\infty} X_k \exp(jk\omega_0 t) \tag{7}$$

[1] With the exception of τ, which obviously cannot be determined from dc measurements.

[2] According to the comments of one reviewer, R_{de}^{-1} varies from zero to 3 mS as the FET is turned on and off by the gate voltage.

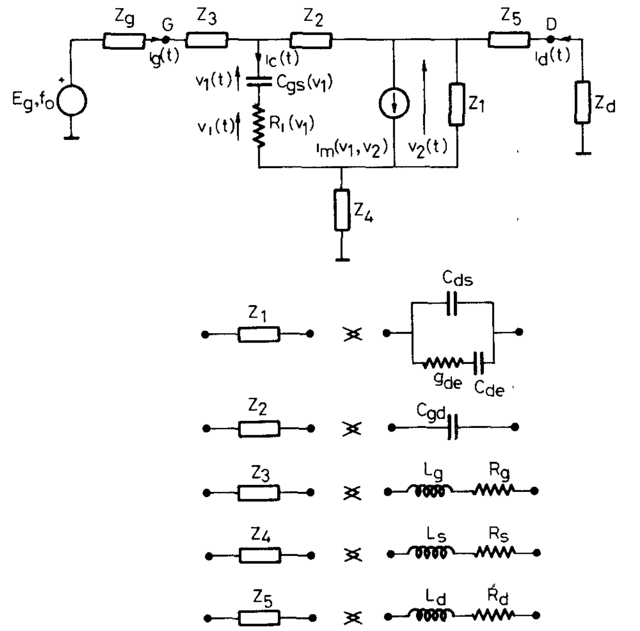

Fig. 3. Large-signal MESFET model under local oscillator excitation.

where $X_{-k} = X_k^*$ since all the functions involved are real, and $f_0 = \omega_0 / 2\pi$ is the LO frequency.[3]

It is straightforward to show that the equations in the frequency domain governing the behavior of the circuit can be expressed as

$$\left.\begin{aligned} V_{1k} &= H_{1k} I_{ck}(V_1) + H_{2k} I_{mk}(V_1, V_2) - V_{ik}(V_1) + E_{1k} \\ &= F_{1k}(V_1, V_2) \\ V_{2k} &= H_{2k} I_{ck}(V_1) + H_{3k} I_{mk}(V_1, V_2) + E_{2k} \\ &= F_{2k}(V_1, V_2) \end{aligned}\right\} \quad \text{for } k = 0, 1, 2, \cdots \tag{8}$$

where

$$V_1 = (V_{10}, V_{11}, V_{12}, \cdots, V_{1k}, \cdots)^{T^4}$$
$$V_2 = (V_{20}, V_{21}, V_{22}, \cdots, V_{2k}, \cdots)^T.$$

Here, V_{1k}, V_{2k}, $I_{ck}(V_1)$, $I_{mk}(V_1, V_2)$, and $V_{ik}(V_1)$ denote the Fourier coefficients of $v_1(t)$, $v_2(t)$, $i_c(t)$, $i_m(t)$, and $v_i(t)$, respectively; $H_{jk} = H_j(k\omega_0)$ (for $j = 1$, 2, and 3); and $E_{mk} = E_m(k\omega_0)$ (for $m = 1$ and 2). The functions $H_j(\omega)$ depend only on the linear part of the circuit, while the functions $E_m(\omega)$ depend, in addition, on the independent LO voltage source.

It should be noted that once V_1 and V_2 are known, the determination of any current or voltage in the circuit requires only linear transformations.

If only the first N harmonics are considered in the analysis, the infinite system given by (8) is reduced to a system consisting of $2(N+1)$ nonlinear complex equations. From a physical standpoint, this truncation is equivalent to short-circuiting the higher harmonic components of $v_1(t)$ and $v_2(t)$.

System (8) can be written as a nonlinear real equation system

$$X = F(X) \tag{9}$$

where

$$X = (x_1, x_2, \cdots, x_{2(2N+1)})^T$$
$$F = (f_1, f_2, \cdots, f_{2(2N+1)})^T$$

with

$$\begin{aligned} x_1 &= V_{10} \\ f_1 &= F_{10} \\ x_{(2N+2)} &= V_{20} \\ f_{(2N+2)} &= F_{20} \end{aligned} \tag{10}$$

and, for $1 \leqslant k \leqslant N$,

$$\begin{aligned} x_{2k} + jx_{2k+1} &= V_{1k} \\ f_{2k} + jf_{2k+1} &= F_{1k} \\ x_{(2N+1)+2k} + jx_{(2N+1)+2k+1} &= V_{2k} \\ f_{(2N+1)+2k} + jf_{(2N+1)+2k+1} &= F_{2k} \end{aligned} \tag{11}$$

and can be solved by using the Newton-Raphson method [14]. Given an initial approximation X_0 to the solution of the system, this iterative method obtains a better X by solving the linear system given by

$$AX = B \tag{12}$$

with

$$A = J(X_0) - I \tag{13}$$
$$B = J(X_0)X_0 - F(X_0) \tag{14}$$

where I and $J(X_0)$ are the identity and Jacobian matrices, respectively. In our case, this has been performed by a standard routine [15].

At the end of the iteration, provided that it converges, the converged vector X can be considered as the solution of (8). Convergence has been achieved in all the cases analyzed when vectors defined by [16]

$$\left.\begin{aligned} V_{1k} &= E_{1k} \\ V_{2k} &= E_{2k} \end{aligned}\right. \quad \text{for } k = 0, 1, \cdots, N \tag{15}$$

were used to initiate the algorithm.

B. Computation of the Jacobian

Despite its excellent convergence characteristics, the major drawback of the Newton-Raphson method when applied to this kind of problem is the high computational cost of the Jacobian. In order to reduce the computer time needed to calculate the elements of the Jacobian, a novel approach [10] has been developed based on that used by Egami [11] and including the modifications introduced in [17]. The application of this approach to the MESFET gate mixer analysis is described as follows.

[3]It is assumed that there are no subharmonic responses and that there is, at least, a stable state.

[4]$()^T$ means transpose of ().

The elements of the Jacobian matrix are computed from
a) for $1 \leqslant m \leqslant 2N+1$, $0 \leqslant k \leqslant N$,

$$\frac{\partial F_{1k}}{\partial x_m} = H_{1k}\frac{\partial I_{ck}(V_1)}{\partial x_m} + H_{2k}\frac{\partial I_{mk}(V_1,V_2)}{\partial x_m} - \frac{\partial V_{ik}(V_1)}{\partial x_m} \tag{16}$$

$$\frac{\partial F_{2k}}{\partial x_m} = H_{2k}\frac{\partial I_{ck}(V_1)}{\partial x_m} + H_{3k}\frac{\partial I_{mk}(V_1,V_2)}{\partial x_m} \tag{17}$$

b) for $2N+2 \leqslant m \leqslant 2(2N+1)$, $0 \leqslant k \leqslant N$,

$$\frac{\partial F_{1k}}{\partial x_m} = H_{2k}\frac{\partial I_{mk}(V_1,V_2)}{\partial x_m} \tag{18}$$

$$\frac{\partial F_{2k}}{\partial x_m} = H_{3k}\frac{\partial I_{mk}(V_1,V_2)}{\partial x_m}. \tag{19}$$

It should be pointed out that it is the computation by finite differences of the derivatives involving the nonlinear characteristics which makes the method prohibitively computer time consuming. Therefore, the main point of the approach is the development of a more elaborated formula for computing such derivatives.

Let us consider first the nonlinear voltage-controlled capacitor $C_{gs}(v_1)$. Its charge–voltage characteristics can be obtained by integrating the expression for the incremental capacitance (2), resulting in

$$q(v_1) = -2\phi C_{gs0}\sqrt{1-\frac{v_1}{\phi}}. \tag{20}$$

Current $i_c(t)$ through this capacitance is given by

$$i_c(t) = \frac{dq[v_1(t)]}{dt}. \tag{21}$$

Then

$$I_{ck} = jk\omega_0 Q_k \tag{22}$$

where I_{ck} and Q_k are the Fourier coefficients of $i_c(t)$ and $q(t)$, respectively.

On the other hand,

$$\frac{\partial q(t)}{\partial x_m} = \sum_{k=-\infty}^{\infty}\frac{\partial Q_k}{\partial x_m}\exp(jk\omega_0 t) \tag{23}$$

and

$$\frac{\partial q(t)}{\partial x_m} = \frac{dq(v_1)}{dv_1}\frac{\partial v_1(t)}{\partial x_m} = C_{gs}(t)\frac{\partial v_1(t)}{\partial x_m} \tag{24}$$

for $1 \leqslant m \leqslant 2N+1$. Differentiation of

$$\begin{aligned} v_1(t) &= \sum_{k=-\infty}^{\infty} V_{1k}\exp(jk\omega_0 t) \\ &= V_{10} + \sum_{k=1}^{\infty}\left(V_{1k}^r + jV_{1k}^i\right)\exp(jk\omega_0 t) \\ &\quad + \sum_{k=1}^{\infty}\left(V_{1k}^r - jV_{1k}^i\right)\exp(-jk\omega_0 t) \end{aligned} \tag{25}$$

yields

$$\frac{\partial v_1(t)}{\partial x_m} = \begin{cases} \dfrac{\partial v_1(t)}{\partial V_{10}} = 1, & m=1 \\ \dfrac{\partial v_1(t)}{\partial V_{1n}^r} = \exp(jn\omega_0 t)+\exp(-jn\omega_0 t), & m=2n \\ \dfrac{\partial v_1(t)}{\partial V_{1n}^i} = j[\exp(jn\omega_0 t)-\exp(-jn\omega_0 t)], & m=2n+1. \end{cases} \tag{26}$$

Therefore,

$$\frac{\partial I_{ck}(V_1)}{\partial x_m} = jk\omega_0\frac{\partial Q_k}{\partial x_m} = \begin{cases} jk\omega_0\dfrac{\partial Q_k}{\partial V_{10}} = jk\omega_0 C_k, & m=1 \\ jk\omega_0\dfrac{\partial Q_k}{\partial V_{1n}^r} = jk\omega_0[C_{k-n}+C_{k+n}], & m=2n \\ jk\omega_0\dfrac{\partial Q_k}{\partial V_{1n}^i} = -k\omega_0[C_{k-n}-C_{k+n}], & m=2n+1 \end{cases} \tag{27}$$

with

$$C_{gs}(t) = \sum_{k=-\infty}^{\infty} C_k\exp(jk\omega_0 t). \tag{28}$$

This expression states that in order to compute all the derivatives associated with this nonlinear element, only the computation of Fourier coefficients for $C_{gs}(t)$ is required.

For $v_i(t)$, considering (4) and by a similar procedure, it is quite straightforward to obtain

$$\frac{\partial V_{ik}(V_1)}{\partial x_m} = \begin{cases} \dfrac{\partial V_{ik}}{\partial V_{10}} = 0, & m=1 \\ \dfrac{\partial V_{ik}}{\partial V_{1n}^r} = jn\omega_0\tau_i\delta_{kn}, & m=2n \\ \dfrac{\partial V_{ik}}{\partial V_{1n}^i} = -n\omega_0\tau_i\delta_{kn}, & m=2n+1 \end{cases} \quad \text{for } 1 \leqslant n \leqslant N \tag{29}$$

where δ_{kn} is the Kronecker symbol and V_{ik} denote the Fourier coefficients of $v_i(t)$.

For the current generator $i_m(t)$, the results are

$$\frac{\partial I_{mk}(V_1,V_2)}{\partial x_m} = \begin{cases} \dfrac{\partial I_{mk}}{\partial V_{10}} = G_{mk}, & m=1 \\ \dfrac{\partial I_{mk}}{\partial V_{1n}^r} = G_{m,k-n}+G_{m,k+n}, & m=2n \\ \dfrac{\partial I_{mk}}{\partial V_{1n}^i} = j[G_{m,k-n}-G_{m,k+n}], & m=2n+1 \end{cases} \tag{30}$$

and

$$\frac{\partial I_{mk}(V_1, V_2)}{\partial x_m} = \begin{cases} \dfrac{\partial I_{mk}}{\partial V_{10}} = G_{dk}, & m = 2N+2 \\ \dfrac{\partial I_{mk}}{\partial V_{2n}^r} = G_{d,k-n} + G_{d,k+n}, & m = 2N+1+2n \\ \dfrac{\partial I_{mk}}{\partial V_{2n}^i} = j[G_{d,k-n} - G_{d,k+n}], & m = 2N+2+2n \end{cases} \tag{31}$$

where $1 \leqslant n \leqslant N$,

$$g_m(t) = \left.\frac{\partial i_m(v_1, v_2)}{\partial v_1}\right|_{(v_1(t-\tau), v_2(t))} = \sum_{k=-\infty}^{\infty} G_{ms}\exp(js\omega_0 t) \tag{32}$$

and

$$g_d(t) = \left.\frac{\partial i_m(v_1, v_2)}{\partial v_2}\right|_{(v_1(t-\tau), v_2(t))} = \sum_{k=-\infty}^{\infty} G_{ds}\exp(js\omega_0 t). \tag{33}$$

The advantage of these formulas is evident: they reduce the calculation of all derivatives to a single computation of the Fourier coefficients for $C_{gs}(t)$, $g_m(t)$, and $g_d(t)$ at each iteration. Obviously, the higher the N, the more important the reduction in the computer time required for computing the Jacobian.

IV. Linear Analysis

Under RF small-signal conditions, the frequencies being present in the mixer are given by

$$f_{k,s} = kf_0 + sf_s \tag{34}$$

with $-\infty \leqslant k \leqslant \infty$ and $s = 0$ and ± 1; f_0 and f_s are the LO and RF frequencies, respectively.

According to this, all the magnitudes in the circuit have the form

$$x(t) = \sum_{k=-\infty}^{\infty} \sum_{s=0,\pm 1} X_{k,s}\exp[j(k\omega_0 + s\omega_s)t] = x_{\mathrm{LO}}(t) + x_{\mathrm{MX}}(t) \tag{35}$$

where

$$x_{\mathrm{LO}}(t) = \sum_{k=-\infty}^{\infty} X_{k,0}\exp(jk\omega_0 t) \tag{36}$$

$$x_{\mathrm{MX}}(t) = \sum_{k=-\infty}^{\infty} \sum_{s=\pm 1} X_{k,s}\exp[j(k\omega_0 + s\omega_s)t]. \tag{37}$$

Obviously, $x_{\mathrm{LO}}(t)$ is the local oscillator component of $x(t)$, while $x_{\mathrm{MX}}(t)$ denotes the small-signal mixing products. Since all the magnitudes involved are real

$$X_{k,s} = (X_{-k,-s})^* \tag{38}$$

it is only necessary to take into consideration one of the two values for s ($s = 1$, for instance).

These coefficients are more conveniently represented in matrix form as follows:

$$\boldsymbol{X} = (X_{-N}, X_{-N+1}, \cdots, X_0, \cdots, X_{N-1}, X_N)^T$$

where the second subscript has been omitted for the sake of simplicity, and it has been assumed that a finite number of components are considered.

It can be shown that the relationship between the mixing products of the voltage and the current across $C_{gs}(v_1)$ can be expressed by

$$\boldsymbol{I}_c = j\boldsymbol{\Omega}\boldsymbol{C}\boldsymbol{V}_1 \tag{39}$$

with

$$\boldsymbol{I}_c = (I_{c,-N}, I_{c,-N+1}, \cdots, I_{c,0}, \cdots, I_{c,N-1}, I_{c,N})^T$$

$$\boldsymbol{V}_1 = (V_{1,-N}, V_{1,-N+1}, \cdots, V_{1,0}, \cdots, V_{1,N-1}, V_{1,N})^T$$

$$\boldsymbol{\Omega} = \begin{bmatrix} \omega_s - N\omega_0 & & & & & & \boldsymbol{0} \\ & \ddots & & & & & \\ & & \omega_s - \omega_0 & & & & \\ & & & \omega_s & & & \\ & & & & \omega_s + \omega_0 & & \\ \boldsymbol{0} & & & & & \ddots & \\ & & & & & & \omega_s + N\omega_0 \end{bmatrix}$$

$$\boldsymbol{C} = \begin{bmatrix} C_0 & & & \cdots & & & \\ & \ddots & & \vdots & & & \\ \cdots & & C_0 & C_1^* & C_2^* & & \cdots \\ \cdots & & C_1 & C_0 & C_1^* & & \cdots \\ \cdots & & C_2 & C_1 & C_0 & & \cdots \\ & & & \vdots & & \ddots & \\ & & & \cdots & & & C_0 \end{bmatrix}.$$

For the resistance $R_i(v_1)$, the relationship is given by

$$\boldsymbol{V}_i = j\tau_i\boldsymbol{\Omega}\boldsymbol{V}_1 \tag{40}$$

with

$$\boldsymbol{V}_i = (V_{i,-N}, V_{i,-N+1}, \cdots, V_{i,0}, \cdots, V_{i,N-1}, V_{i,N})^T$$

while that for the current generator $i_m(v_1, v_2)$ has the following form:

$$\boldsymbol{I}_m = \boldsymbol{G}_m\boldsymbol{T}\boldsymbol{V}_1 + \boldsymbol{G}_d\boldsymbol{V}_2 \tag{41}$$

with

$$\boldsymbol{I}_m = (I_{m,-N}, I_{m,-N+1}, \cdots, I_{m,0}, \cdots, I_{m,N-1}, I_{m,N})^T$$

$$\boldsymbol{V}_2 = (V_{2,-N}, V_{2,-N+1}, \cdots, V_{2,0}, \cdots, V_{2,N-1}, V_{2,N})^T$$

$$\boldsymbol{G}_m = \begin{bmatrix} G_{m0} & & & \cdots & & & \\ & \ddots & & \vdots & & & \\ \cdots & & G_{m0} & G_{m1}^* & G_{m2}^* & & \cdots \\ \cdots & & G_{m1} & G_{m0} & G_{m1}^* & & \cdots \\ \cdots & & G_{m2} & G_{m1} & G_{m0} & & \cdots \\ & & & \vdots & & \ddots & \\ & & & \cdots & & & G_{m0} \end{bmatrix}$$

$$\boldsymbol{T} = \begin{bmatrix} \exp[j(\omega_s - N\omega_0)\tau] & & \mathbf{0} \\ & \exp[j\omega_s\tau] & \\ \mathbf{0} & & \exp[j(\omega_s + N\omega_0)\tau] \end{bmatrix}$$

$$\boldsymbol{G}_d = \begin{bmatrix} G_{d0} & & & \cdots & & & \\ & \ddots & & \vdots & & & \\ \cdots & & G_{d0} & G_{d1}^* & G_{d2}^* & & \cdots \\ \cdots & & G_{d1} & G_{d0} & G_{d1}^* & & \cdots \\ \cdots & & G_{d2} & G_{d1} & G_{d0} & & \cdots \\ & & & \vdots & & \ddots & \\ & & & \cdots & & & G_{d0} \end{bmatrix}.$$

For the mixing products, the equations imposed by the circuit can be written in matrix form as follows:

$$\begin{aligned} \boldsymbol{V}_1 &= \boldsymbol{H}_1\boldsymbol{I}_c + \boldsymbol{H}_2\boldsymbol{I}_m - \boldsymbol{V}_i + \boldsymbol{E}_1' \\ \boldsymbol{V}_2 &= \boldsymbol{H}_2\boldsymbol{I}_c + \boldsymbol{H}_3\boldsymbol{I}_m + \boldsymbol{E}_2' \end{aligned} \tag{42}$$

with

$$\boldsymbol{E}_m' = (E_m'(\omega_s - N\omega_0), \cdots, E_m'(\omega_s), \cdots, E_m'(\omega_s + N\omega_0))^T \quad \text{for } m = 1 \text{ and } 2$$

$$\boldsymbol{H}_j = \begin{bmatrix} H_j(\omega_s - N\omega_0) & & \mathbf{0} \\ & H_j(\omega_s) & \\ \mathbf{0} & & H_j(\omega_s + N\omega_0) \end{bmatrix} \quad \text{for } j = 1, 2, \text{ and } 3$$

and where $E_m'(\omega)$ depend on the linear part of the circuit and on the independent voltage source.

Equations (39)–(41) in conjunction with the system (42) yield the following conversion system:

$$\begin{aligned} &(\boldsymbol{I} - j\boldsymbol{H}_1\boldsymbol{\Omega}\boldsymbol{C} - \boldsymbol{H}_2\boldsymbol{G}_m\boldsymbol{T} + j\tau_i\boldsymbol{\Omega})\boldsymbol{V}_1 - \boldsymbol{H}_2\boldsymbol{G}_d\boldsymbol{V}_2 = \boldsymbol{E}_1' \\ &(-j\boldsymbol{H}_2\boldsymbol{\Omega}\boldsymbol{C} - \boldsymbol{H}_3\boldsymbol{G}_m\boldsymbol{T})\boldsymbol{V}_1 + (\boldsymbol{I} - \boldsymbol{H}_3\boldsymbol{G}_d)\boldsymbol{V}_2 = \boldsymbol{E}_2'. \end{aligned} \tag{43}$$

Once vectors $\boldsymbol{V}_1$ and $\boldsymbol{V}_2$ are determined, terminal currents $\boldsymbol{I}_g$ and $\boldsymbol{I}_d$ (see Fig. 2) can be easily computed by the formulas

$$\begin{aligned} \boldsymbol{I}_g &= (\boldsymbol{Y}_2 + j\tau_i\boldsymbol{Y}_2\boldsymbol{\Omega} + j\boldsymbol{\Omega}\boldsymbol{C})\boldsymbol{V}_1 - \boldsymbol{Y}_2\boldsymbol{V}_2 \\ \boldsymbol{I}_d &= (-\boldsymbol{Y}_2 - j\tau_i\boldsymbol{Y}_2\boldsymbol{\Omega} + \boldsymbol{G}_m\boldsymbol{T})\boldsymbol{V}_1 + (\boldsymbol{Y}_1 + \boldsymbol{Y}_2 + \boldsymbol{G}_d)\boldsymbol{V}_2 \end{aligned} \tag{44}$$

with

$$\boldsymbol{Y}_j = \begin{bmatrix} Y_j(\omega_s - N\omega_0) & & \mathbf{0} \\ & Y_j(\omega_s) & \\ \mathbf{0} & & Y_j(\omega_s + N\omega_0) \end{bmatrix} \quad Y_j = Z_j^{-1} \text{ for } j = 1 \text{ and } 2$$

$$\boldsymbol{I}_g = (I_{g,-N}, \cdots, I_{g,0}, \cdots, I_{g,N})^T$$

$$\boldsymbol{I}_d = (I_{d,-N}, \cdots, I_{d,0}, \cdots, I_{d,N})^T.$$

The mixer is considered as a two-port circuit (input: RF at gate; output: IF at drain), its behavior being controlled by the terminations at gate and drain (common-source configuration has been assumed) at the remaining mixing product frequencies. If S parameters are chosen to describe the behavior of this two-port circuit, the conversion gain and stability of the mixer can be easily analyzed by employing the well-established S-parameter theory mainly used in the design of microwave amplifiers.

Computation of S parameters for given terminations at the parasitic frequencies requires the linear analysis to be performed twice, once with the RF source at the gate, and again with the IF source at the drain. It should be noted that, unless a multiterminal S matrix is used, this calculation has to be performed every time modifications in the termination at the parasitic frequencies are introduced.

V. Conversion Gain and Stability in an X-Band MESFET Gate Mixer

In this section, the nonlinear–linear analysis technique previously developed is applied to the study of the conversion gain and stability of an X-band MESFET gate mixer. The LO frequency, RF, and IF chosen are 11.0, 12.0, and 1.0 GHz, respectively. The dc bias voltages are $V_{GS} = -0.9$ V and $V_{DS} = 3.0$ V, near the "knee" of the I_{DS}–V_{GS} characteristics.

A. Conversion Gain and Stability

In the analysis of the LO injection, only the fundamental frequency has been taken into consideration. The Newton-Raphson algorithm has required 2–8 iterations to calculate the response depending on the input power level.

In the linear analysis, only the RF, IF, and image (IM) frequencies have been taken into consideration. A preliminary analysis of the influence of the terminations at these three frequencies at both drain and gate ports showed that the influence of the image frequency at both ports on the conversion gain is negligible, so subsequently short-circuit terminations will be assumed for this frequency at both ports. Therefore, the mixer performance is mainly controlled by the IF and RF terminations at gate and drain.

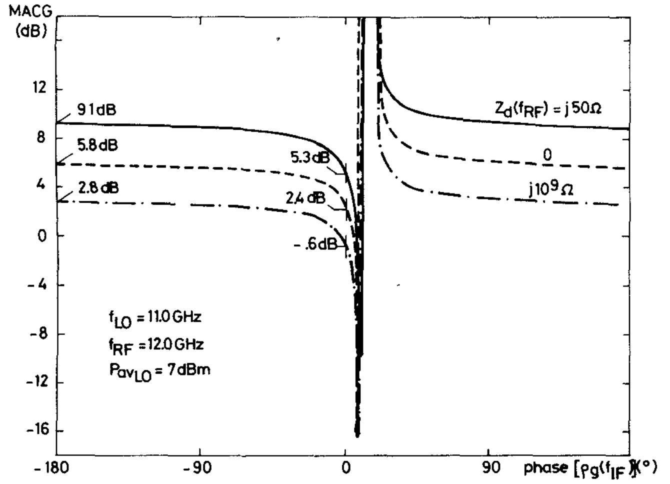

Fig. 4. Maximum available conversion gain (MACG) versus phase [$\rho_g(f_{IF})$] with $Z_g(f_{IM}) = Z_d(f_{IM}) = 0$ for three different values of $Z_d(f_{RF})$.

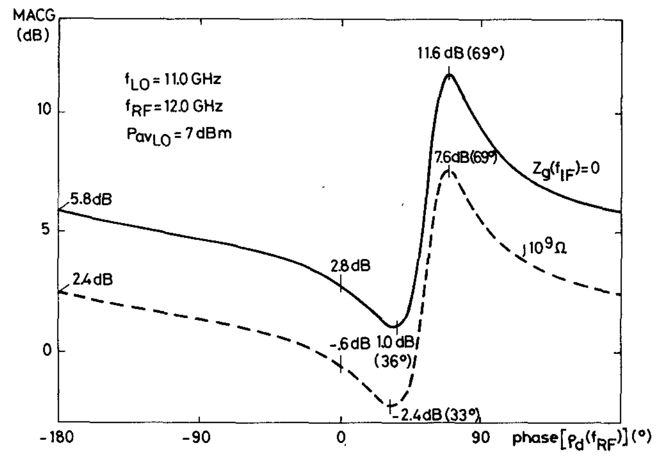

Fig. 5. Maximum available conversion gain (MACG) versus phase [$\rho_d(f_{RF})$] with $Z_g(f_{IM}) = Z_d(f_{IM}) = 0$ for two different values of $Z_g(f_{IF})$.

Fig. 4 shows the value of the maximum available conversion gain (MACG) versus the phase of the gate termination reflection coefficient at the IF for three different values of $Z_d(f_{RF})$ (see Fig. 3). Only pure reactive terminations are considered. It should be noted that the use of this representation (the phase of the reflection coefficient instead of the value of the imaginary part of the impedance, as has been employed by other authors [4], [6]) provides a much more precise idea of the sensitivity of the MACG, especially in considering the possibility of improving the mixer conversion gain by an appropriate choice of the terminations at the parasitic frequencies. The results shown in this figure indicate that the mixer becomes unstable for the values of phase [$\rho_g(f_{IF})$] lying in the proximity of the open circuit, while outside this region the MACG remains nearly constant.

In Fig. 5, the value of the MACG versus the phase of the drain termination reflection coefficient at the RF for two different values of $Z_g(f_{IF})$ is shown. It can be seen in this figure that there is a 10-dB variation in the MACG depending on the value of phase [$\rho_d(f_{RF})$]. A more detailed analysis shows that the peak in the MACG transforms into an unstable region for lower values of L_s ($L_s = 0.06$ nH in this analysis).

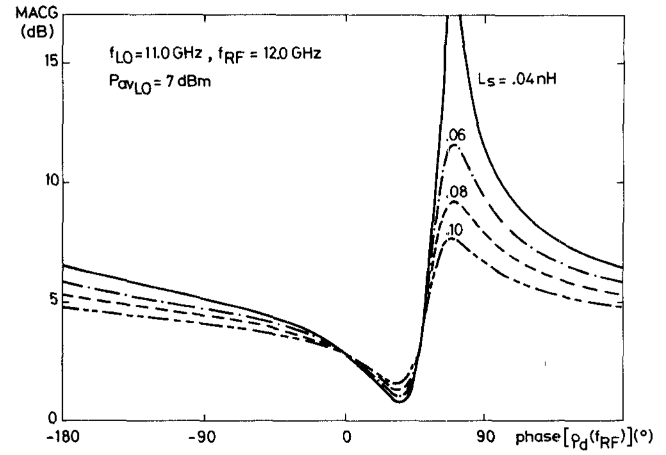

Fig. 6. Maximum available conversion gain (MACG) versus phase [$\rho_d(f_{RF})$] with $Z_g(f_{IF}) = Z_g(f_{IM}) = Z_d(f_{IM}) = 0$ for four different values of L_s.

To summarize, there exist two unstable regions controlled by the IF and RF terminations at gate and drain ports, respectively, which suggests the possibility of increasing the conversion gain by an appropriate choice of these terminations. However, only the drain termination at the RF allows this improvement without significantly degrading the overall performance of the mixer.

B. Influence of Model Elements

A study [18] using the described model and analysis technique of the influence of model elements on the mixer performance has confirmed that the two unstable regions are mainly due to the feedback introduced by C_{gd} [6]. Nevertheless, the one controlled by the drain termination at the RF is the result of the combined effect of C_{gd} and L_s. In fact this unstable region can disappear for some values of L_s, as is clearly seen in Fig. 6. On the other hand, the effect of the nonlinearity $C_{gs} - R_i$ is of second order when compared to elements L_s and C_{gd}, and therefore it can be ignored in any approximate analysis of the mixer conversion gain.

C. Improvement of the Conversion Gain

From a design point of view, the combination short-circuit/short-circuit ($Z_g(f_{IF})/Z_d(f_{RF})$) provides a good tradeoff between conversion gain and stability. In fact this combination has been considered as optimum by different authors [3], [4], [6]. However there exists the possibility of drastically increasing the conversion gain by a proper choice of the drain termination at the RF. The viability of this solution depends on the effect of this impedance on the reflection coefficients which provide conjugate matching, and on the associated noise figure.

In Fig. 7, the magnitudes of these reflection coefficients and the associated conversion gain versus phase [$\rho_d(f_{RF})$] for $Z_g(f_{IF})$ = short circuit are shown. These results indicate that conjugate matching at the IF is easy to achieve

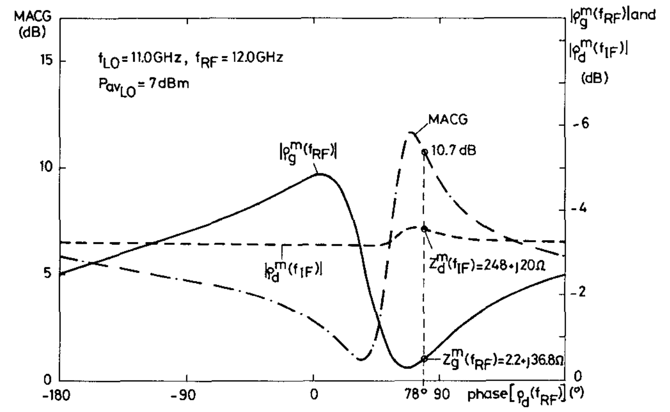

Fig. 7. Maximum available conversion gain (MACG) and conjugate matching reflection coefficients versus phase $[\rho_d(f_{RF})]$ with $Z_g(f_{IF}) = 0$.

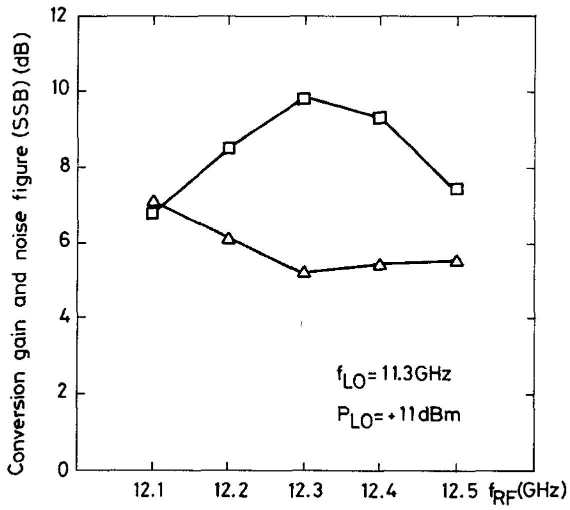

Fig. 8. Experimental conversion gain (□) and SSB noise figure (△) versus frequency.

independently from the value for $Z_d(f_{RF})$. On the contrary, the gate reflection coefficient at RF providing conjugate matching not only depends strongly on $Z_d(f_{RF})$, but becomes very high near the peak of the gain, making the synthesis of the input circuit very critical. For instance, for phase $[\rho_d(f_{RF})] = 78°$ (see Fig. 7) the MACG is 10.7 dB, i.e., an improvement of about 5 dB with respect to the short-circuit/short-circuit termination, while the impedances which provide conjugate matching are $Z_g^m(f_{IF}) = 248 + j20\ \Omega$ and $Z_d^m = 2.2 + j36.8\ \Omega$, the latter being practically in the limit of the impedance achievable using microstrip technology. Nevertheless if the matching becomes too critical it is always possible to slightly reduce the conversion gain in order to facilitate its manufacture.

On the other hand it is seen in Fig. 4 that there is no possibility of improving the conversion gain by varying $Z_g(f_{IF})$, and that the best choice for this termination is a short circuit.

Finally as far as the noise figure is concerned, its calculation is not within the scope of this paper. Nevertheless, Tie *et al.* [6], [7] have shown that short-circuiting the IF gate termination provides good noise figure performance. This criterion is also shared by Maas [19] and Ohnishi *et al.* [20]. With this short circuit at the IF gate port, the mixer noise figure, for a given LO injection level, decreases when the conversion gain increases as $Z_d(f_{RF})$ is varied [6]. Therefore, it is reasonable to predict that the overall performance (conversion gain and noise figure) of the mixer can be improved by a proper choice of $Z_d(f_{RF})$.

VI. *X*-Band Mixer Design and Performance

In order to check experimentally the validity of the conclusions previously obtained, an *X*-band gate mixer was designed, fabricated, and measured.

The mixer was designed for operation at 12.3 GHz with 1.0 GHz IF and 11.3 GHz LO, with the device biased near pinchoff ($V_{GS} = -0.75$ V, $V_{DS} = 3.0$ V). For optimum conversion gain, the input network must provide conjugate matching at the RF and a short circuit at the IF, while the output network must conjugate match the device at the IF and synthesize the desired value for $Z_d(f_{RF})$. For the LO level which drives the device into the region of positive values for $v_1(t)$, the value of $Z_d(f_{RF})$ corresponding to the peak value of the MACG ($\simeq 11$ dB) is $Z_{d(\text{optimum})} \cong j73\ \Omega$. Considering that for $Z_d(f_{RF}) = 0$ the MACG is about 6 dB, the theoretical improvement is about 5 dB.

The circuit was fabricated on a 1 in × 1 in 25-mil-thick alumina substrate using microstrip technology. Frequency dispersion effects and discontinuities were taken into consideration [21]. For the input network, a shorted stub one quarter wavelength long at the RF realizes an impedance that approximates a short circuit at the IF. A three-section quarter-wave transformer provided conjugate matching at the RF after removing the imaginary part of the impedance presented by the device. No attempt was made to match the local oscillator frequency. Therefore, the mixer required more LO power than necessary. For the output network, the desired impedance at RF was obtained by a short circuit realized by a quarter-wave open-circuited stub. Conjugate matching at the IF was achieved by means of a series lumped inductance. Bias voltages were introduced by using external bias T networks.

The conversion gain and the noise figure of the mixer were measured employing an experimental arrangement based on the HP 8970 automatic noise figure meter. Nevertheless independent measurements of the conversion gain at RF and the image frequency were also performed using a spectrum analyzer. The image frequency conversion gain was at least 9 dB less than the RF gain.

The experimental results are shown in Figs. 8 and 9. The mixer exhibits a conversion gain greater than 7 dB and a noise figure (SSB) ranging from 5 to 7 dB over 400 MHz. At the center frequency (12.3 GHz), the conversion gain and the noise figure (SSB) are 9.8 and 5.2 dB, respectively. Fig. 10 shows the close agreement of experimental and model-predicted results. An improvement can be appreciated (about 5 dB for $P_{LO} \simeq 11$ dBm) in the conversion gain achieved by the proper termination of the RF at the drain port. The influence of the drain termination at the LO frequency can also be seen. The main effect of not short-

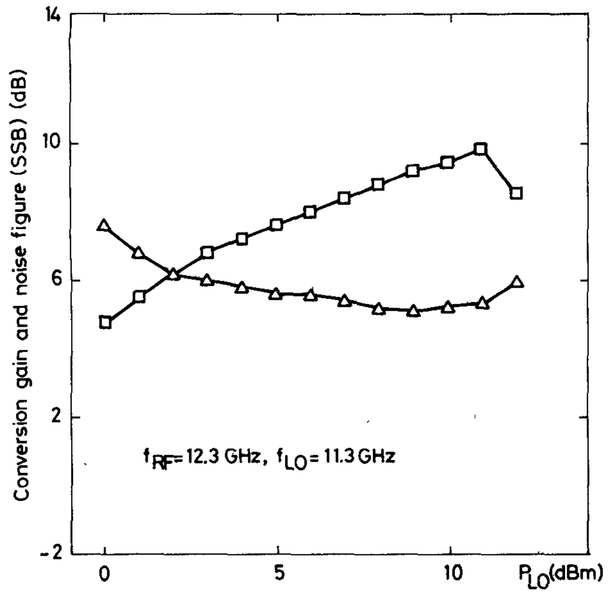

Fig. 9. Experimental conversion gain (□) and SSB noise figure (△) versus local oscillator power.

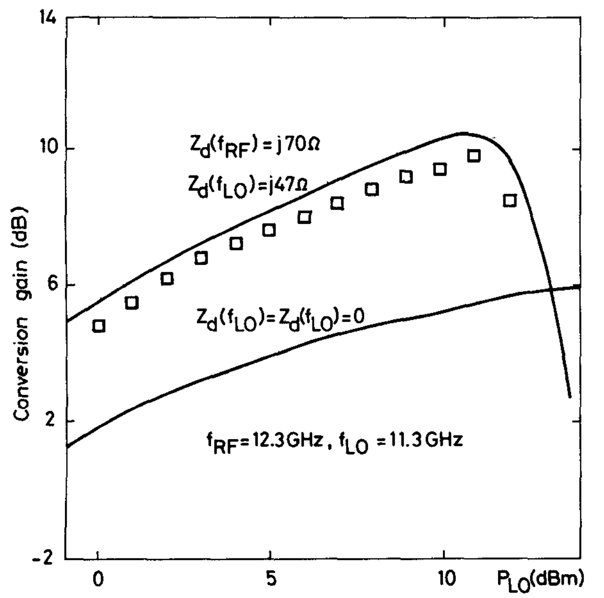

Fig. 10. Measured (□) and predicted (solid lines) conversion gain versus local oscillator power.

circuiting the drain port at the LO frequency is to make the voltage $v_2(t)$ reach the nonsaturation region, which leads to a drop in the conversion gain for high LO power levels.

VII. Conclusions

A mathematical tool for a more complete and efficient analysis of MESFET mixers has been developed. Both nonlinear and linear analyses have been taken into consideration. A novel approach for solving the nonlinear problem in the frequency domain which reduces computational time has been presented. The use of matrix notation in conjunction with the S-parameter-based study of the mixer conversion gain and stability avoids unnecessary and cumbersome algebraic manipulations.

This nonlinear/linear analysis technique has been applied to the study of the performance of an X-band MESFET gate mixer. The main results obtained relate to the existence of two unstable regions in the mixer, controlled by the drain and gate terminations at the RF and IF respectively. The characteristics of these regions are similar to those described by other authors [4], [6]. The possibility of improving the conversion gain by an appropriate choice of the drain termination at the RF has been theoretically and experimentally demonstrated. Using this method, an X-band MESFET gate mixer with state-of-the-art performance has been designed and fabricated.

Although only MESFET gate mixers have been studied, the method can be used for the analysis of any other MESFET configuration if improved MESFET models, capable of, for instance, simulating the device behavior in the nonsaturation region, are considered. The method can also be easily extended to the analysis of dual-gate and distributed MESFET mixers.

Acknowledgment

Thanks are expressed to Dr. O. S. A. Tang for many valuable discussions and suggestions and to Dr. G. Lambrianou, C. L. Law, Dr. M. N. Bukhari, and K. Smith for helpful assistance.

References

[1] R. A. Pucel, D. Masse, and R. Bera, "Performance of GaAs MESFET mixers at X-band," *IEEE Trans. Microwave Theory Tech.*, vol. MTT-24, pp. 251–360, June 1976.

[2] O. Kurita and K. Morita, "Microwave MESFET mixer," *IEEE Trans. Microwave Theory Tech.*, vol. MTT-24, pp. 361–366, June 1976.

[3] P. Harrop and T. A. C. M. Claasen, "Modelling of an F.E.T. mixer," *Electron. Lett.*, vol. 14, no. 12, pp. 369–370, 1978.

[4] G. Begemann and A. Hecht, "The conversion gain and stability of MESFET gate mixers," in *Proc. 9th European Microwave Conf.*, 1979, pp. 316–320.

[5] G. Begemann and A. Jacob, "Conversion gain of MESFET drain mixers," *Electron. Lett.*, vol. 15, no. 18, pp. 567–568, 1979.

[6] G. K. Tie, "Conversion gain and noise performance of a microwave FET mixer," Ph.D. dissertation, Department of Electronics, Chelsea College, University of London, 1983.

[7] G. K. Tie and C. S. Aitchison, "Noise figure and associated conversion gain of a microwave MESFET gate mixer," in *Proc. 13th European Microwave Conf.*, 1983, pp. 579–584.

[8] S. A. Maas, "Theory and analysis of GaAs MESFET mixers," *IEEE Trans. Microwave Theory Tech.*, vol. MTT-32, pp. 1402–1406, Oct. 1984.

[9] J. Dreifuss, A. Madjar, and A. Bar-Lev, "A novel method for the analysis of microwave two-port active mixers," *IEEE Trans. Microwave Theory Tech.*, vol. MTT-33, pp. 1241–1244, Nov. 1985.

[10] C. Camacho-Peñalosa, "Numerical steady-state analysis of nonlinear circuits driven by multi-tone signals," to be published.

[11] S. Egami, "Nonlinear, linear analysis and computer-aided design of resistive mixers," *IEEE Trans. Microwave Theory Tech.*, vol. MTT-22, pp. 270–275, Mar. 1974.

[12] Y. Tajima, B. Wrona, and K. Mishima, "GaAs FET large-signal model and its application to circuit designs," *IEEE Trans. Electron Devices*, vol. ED-28, pp. 171–175, Feb. 1981.

[13] C. Camacho-Peñalosa and C. S. Aitchison, "Modelling frequency dependence of output impedance of a microwave MESFET at low frequencies," *Electron. Lett.*, vol. 21, pp. 528–529, 1985.

[14] B. P. Demidovich and I. A. Maron, Cálculo numérico fundamental. Madrid: Paraninfo, 1977.

[15] *UNIVAC Large Scale Systems MATH-PACK*, Sperry Rand Corporation, 1973.

[16] C. Camacho-Peñalosa, "Numerical steady-state analysis of nonlinear microwave circuits with periodic excitation," *IEEE Trans. Microwave Theory Tech.*, vol. MTT-31, pp. 724–730, Sept. 1983.
[17] C. Camacho-Peñalosa, L. Mariscal-Rico, and A. Alonso-Pardo, "Efficient calculation of partial derivatives in nonlinear conductances driven by periodic input signals," to be published.
[18] C. Camacho-Peñalosa, "Sobre el análisis de mezcladores de microondas con transistores MESFET," in *Proc. 2° Simp. Electrónica Telecomunicações* (Lisboa), 1986, pp. 405–408.
[19] S. A. Maas, "Design and performance of a 45-GHz HEMT mixer," *IEEE Trans. Microwave Theory Tech.*, vol. MTT-34, pp. 799–803, July 1986.
[20] H. Ohnishi and S. Yamashita, "*S*- and *X*-band GaAs FET mixers with thin-film lumped elements," *IEEE Trans. Microwave Theory Tech.*, vol. MTT-32, pp. 135–138, Jan. 1984.
[21] K. C. Gupta, R. Garg, and R. Chadha, *Computer-Aided Design of Microwave Circuits.* Norwood, MA: Artech House, 1981.

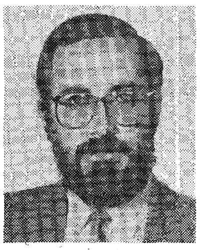

Carlos Camacho-Peñalosa (S'80–M'82) was born in Sevilla, Spain, in 1954. He received the Ingeniero de Telecomunicación degree in 1976 and the Doctor degree in 1982, both from the Universidad Politécnica de Madrid, Spain.

Since 1976, he has been with the ETSI Telecomunicación, Universidad Politécnica de Madrid, as a Research Assistant, Assistant Professor, and Associate Professor. In 1985, he was appointed Profesor Titular at the Universidad Politécnica de Madrid. During the period from September 1984 to July 1985, he was a Visiting Researcher in the Department of Electronics, Chelsea College (now called King's College), University of London, England. His research interests include microwave solid-state circuits, nonlinear systems, and electromagnetics.

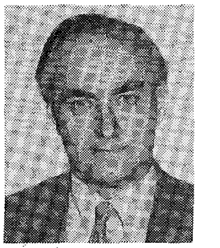

Colin S. Aitchison was born in Morecambe, England, in 1933. He received the B.Sc. and A.R.C.S. degrees in physics from Imperial College, London University, London, England, in 1955.

He worked for Philips Research Laboratories, Redhill, Surrey, England, from 1955 to 1972, being initially concerned with the noise-reduction properties of direct injection phase-locked klystrons for use with Doppler radars. He led a group concerned with parametric amplifiers, mixers, ferrite limiters, lumped microwave components, and Gunn and avalanche oscillators. In 1972, he joined the Department of Electronics, Chelsea College, University of London, where he was Professor of Electronics. He has recently joined ERA Technology Ltd. at Leatherhead, Surrey, England. His research interests remain in the field of active microwave circuits, particularly distributed amplifiers.

Professor Aitchison is a Fellow of the Institute of Electrical Engineers, a member of the Institute of Physics, and an Emeritus Professor of the University of London.